A Free Space Optical Link in a Laboratory Environment

Ahmed F. Hussein, Ahmed Abd El Aziz, Heba A. Fayed, and Moustafa A. Aly

Photonics Research Laboratory (PRL), Arab Academy for Science and Technology, Alexandria, Egypt

ahmed.fahmy.hussein@gmail.com, ahmedabdelazizyoussef@gmail.com, hebam@aast.edu, drmosaly@gmail.com

Abstract— **This paper implements an experimental free space optical 1 m link. A simple low speed transmitter and a receiver are designed and implemented, and then the received voltage is measured. An investigation for different noise effects is conducted in a simulation for the transmission link. Theoretical bit error rate (BER) is calculated at the track end by eye diagram analysis and then compared with the simulation optical sensitivity at BER of 10^{-9}. A reliable link is obtained at data rates ranging from 512 kb/s up to 5 Mb/s according to the available data source and can be extended to higher data rates. A clear wide eye pattern is obtained with theoretical BER ≤ 10^{-9}.**

Keywords— **Free Space Optics (FSO), Infrared (IR), Light Emitting Diode (LED), photodiode, Transimpedance Amplifier (TIA)**

I. INTRODUCTION

For the last thirty years, high achievements and breakthroughs have been made in the field of free space optical (FSO) communications. The interest in such a field besides the military applications includes and is not limited to common appliances such as telephones and computer systems, satellite communications, ground-to-train links, last mile access, cellular communications and optical fiber back up links.

The electromagnetic spectrum has been congested with all the surrounding technologies leaving a narrow space for a new one. An optical carrier frequency ranges from 10^{12}-10^{16} Hz, and thus permits data bandwidth up to 2000 THz [1]. FSO is a line of sight technology which allows frequency reuse, where the band is unlicensed. Moreover, thousands of channels can be added without interference only using different wavelength sources [2]. For the previous reasons, FSO is an attractive ongoing research point.

In this paper a short optical through air link is studied. A ray trace model including noise analysis is investigated in Sec. II. In Sec. III, the communication system including the transmitter and receiver designs is presented. Results are shown in Sec. IV followed by concluding the paper in Sec. V.

II. PROPOSED SYSTEM

In this section a block diagram for the implemented FSO link is presented in Fig. (1). Random input data is generated using a pseudorandom source with a length of (210-1) before entering the transmitter to modulate an infrared (IR) LED using a non-return-to-zero (NRZ) on-off-keying (OOK). The data rate is limited to 5 Mb/s because of the available pseudorandom source; however the experiment is tested for two more different data rates: 512 kb/s and 1 Mb/s. A LED driver circuit controls the on-off biasing current that feeds a 50 mW-LED. Incident light is collimated through a 5.5 cm lens to an infrared filtered PIN photodiode. Light pulses are

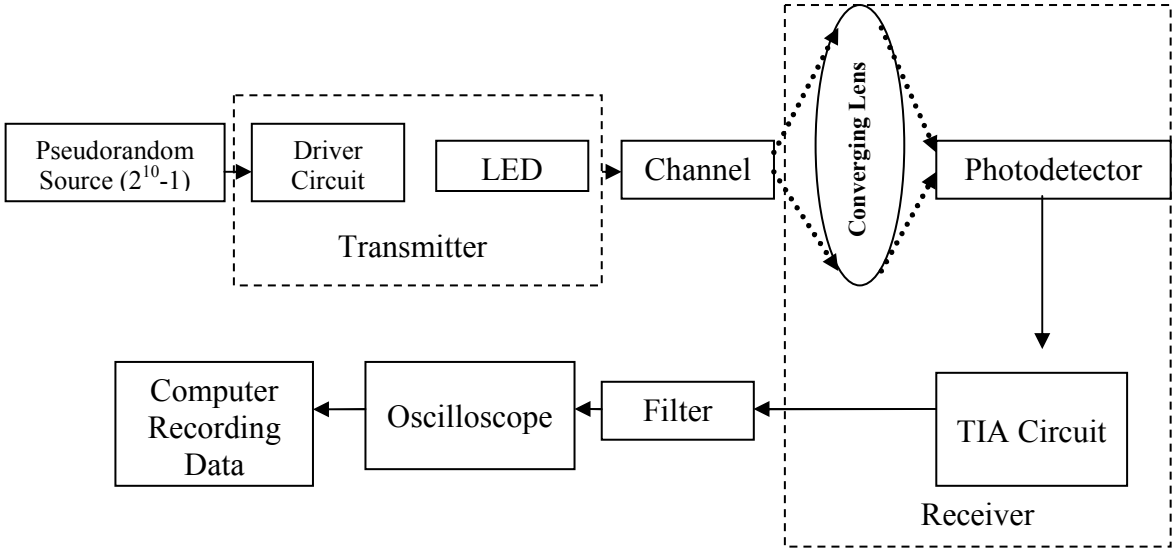

Figure 2. Proposed system block diagram

978-1-4673-9572-4/15/$31.00 ©2015 IEEE

then converted into nA-current values which are amplified into detectable voltage using a transimpedance amplifier (TIA). A digital storage oscilloscope (DSO) saves the received signal frames.

A. Ray Trace Model

In order to trace the received power and compare it with the experimental results, a ray trace model following the Lambertian source model; presented in [3], is implemented. This is governed by the following Eq. (1),

$$P_R = \frac{1}{d^2}\frac{n+1}{2\pi} P_E \cos^{n+1}\varphi A_r \, rect(\frac{\varphi}{FOV}) \quad (1)$$

where P_R is the received power, P_E is the transmitted power, d is the distance between the transmitter and receiver, n is the order of emission, φ is the angle of incidence, A_r is the physical effective area of the photodiode and FOV is the receiver field of view.

B. Photodetection Noise

A digital communication system performance highly depends on its noise analysis. In this study, photodetection noise plays an important role in the quality of the received signal. The following study is inherited from the photodiode characteristics found in [1] and [4].

***1) Photon fluctuation noise*:** This type of noise results from the quantum nature of light, where the actual number of emitted photons from a source per second follows the poisson's distribution. The quantum shot noise variance (σ^2_{qtm}) can be obtained from the following relation,

$$\sigma^2_{qtm} = 2qi_{ph}B \quad (2)$$

Where q is the electron charge constant, i_{ph} is the photon generated current and B is the electric bandwidth in Hz.

2) *Dark Current Noise*: When no photons hit the photodiode, a leakage current (i_{dk}) between 1 and 10 nA is generated in case of silicon photodiodes. This current is not useful, and thus generates a shot noise (σ^2_{dk}) as shown,

$$\sigma^2_{dk} = 2qi_{dk}B \quad (3)$$

3) *Background Radiation*: This type of noise results from other sources of light surrounding the receiver including: the sky, the sun and different indoor light emissions. This type of noise is reduced by using optical bandpass filters and can be neglected when the experiment is held indoors in a dark room as in this paper scope.

4) *Thermal Noise*: This type of noise is caused by the electrons fluctuations in a receiver circuitry. The thermal noise variance (σ^2_{th}) is affected by the equivalent resistance (R_L) and the temperature (T). This part of study is influenced by further circuit analysis inherited from [5] and governed by the following main equation,

$$\sigma^2_{th} = \frac{4kTB}{R_L} \quad (4)$$

C. Performance measurement

Experimental performance can be measured by comparison with expected simulation results, in addition to statistical BER deduction from the recorded samples as follows,

$$Q = \frac{\mu_1 - \mu_0}{\sigma_1 + \sigma_0} \quad (5)$$

$$BER = \frac{1}{2} erfc(\frac{Q}{\sqrt{2}}) \approx \frac{\exp(\frac{-Q^2}{2})}{Q\sqrt{2\pi}} \quad (6)$$

Where $\mu_{1/0}$ and $\sigma_{1/0}$ are respectively, the current means and variances for both "1" and "0" bits, Q is a signal to noise ratio measure and erfc(.) is the well known complementary error function in statistics [6].

III. Experimental Demonstration

A 1 m track is implemented to vary the distance between both the transmitter and the receiver in 5 cm steps. At each step, the received pulses are recorded via DSO to computer, then filtered and finally peak to peak voltage is measured. The transmitter and receiver designs are based on [7].

A. Transmitter Design

The schematic for the circuit presented in Fig. (1) shows a low speed transmitter design. The main function of this circuit is to provide a constant current regardless the voltage fluctuations where the emitted power varies with the current value. The positive pin of the op amp is fed by the input pseudorandom voltage. From the BJT datasheet [8], the minimum value for the base emitter voltage ON state (V_{BE}) is 0.75 V. The maximum op amp output swing according to the datasheet [9], is 3.7 V, which puts a restriction on the maximum emitter voltage ($V_{E-\max}$) not to exceed 2.95 V for the input voltage (V_{in}) above 2.95 V. The emitter resistance (R_E) is chosen to be 36.4 Ω. According to the following LED current (I_{LED}) equations, $I_{LED-\max}$ equals 81 mA which does not exceed the maximum allowable current in [10].

$$I_{LED} = \frac{2.95}{R_E}, \mathrm{V_{in}} > 2.95\,\mathrm{V} \quad (7)$$

$$I_{LED} = \frac{\mathrm{V_{in}}}{R_E}, 0\,\mathrm{V} \le \mathrm{V_{in}} \le 2.95\,\mathrm{V} \quad (8)$$

Decoupling capacitors are used near op amp power pins to short high frequency noise and voltage source is decoupled to reduce voltage drooping due to high switching frequencies.

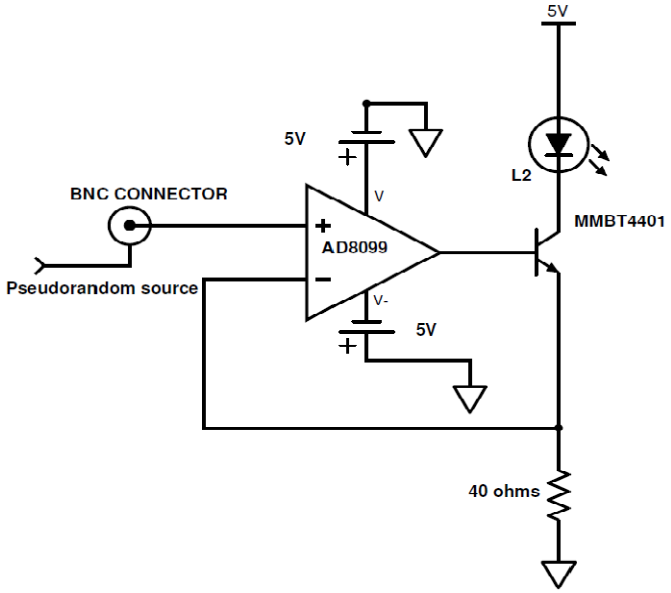

Figure 2. Transmitter circuit

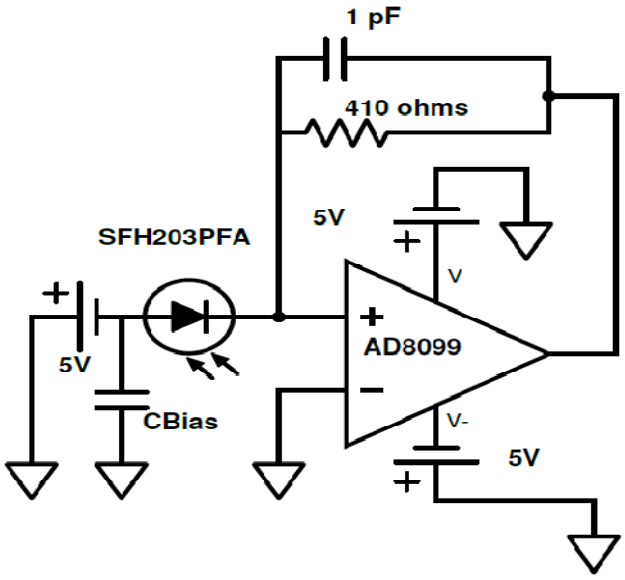

Figure 3. Receiver circuit

B. Receiver Design

The main function of the receiver circuit is to detect optical signals. A lens converges optical pulses onto the photodetector surface. Optical pulses are converted into current which in turn is converted into voltage and saved using an oscilloscope interface to computer. A digital low pass filter removes unwanted noise from saved samples and theoretical BER is calculated then compared with the intended optical sensitivity.

The presented schematic in Fig. (3) shows an IR filtered photodiode with a maximum spectral sensitivity in the range 700-1100 nm [11]. The circuit acts as a transimpedance amplifier that converts the current generated by the photodiode to detectable voltage values with an amplification factor equal to the feedback resistance (R_F). This method is preferred in high speed applications more than conversion using a simple large resistor to reduce the effect of photodiode capacitance, and thereby bandwidth increases. Another advantage is to reduce the loading effect due to the low output impedance of the op amp which makes it suitable to a wide variety of loads [2]. The bias capacitor (C_{Bias}) reduces the noise from the bias voltage connected to the photodiode. The feedback capacitor (C_F) is responsible for preventing the self oscillations and ensure stability by compensating the input capacitance according to the following relation described in [7],

$$C_F = \frac{1}{4\pi R_F GBW}\left[1+\sqrt{1+8\pi R_F C_D GBW}\right] \quad (9)$$

where, GBW is the gain bandwidth product of the op amp and C_D is the sum of the input capacitance resulting from the photodiode and the op amp terminals.

IV. Results and Discussion

The voltage measurement starts at a distance 10 cm between the transmitter and the receiver (i.e. the minimum distance that can be obtained by the structure) with a step size of 5 cm till the end of the 1 m track. As shown in Fig. 4, the received voltage follows the Lambertian ray trace model. The simulated voltage exhibits a near response to the experimental results.

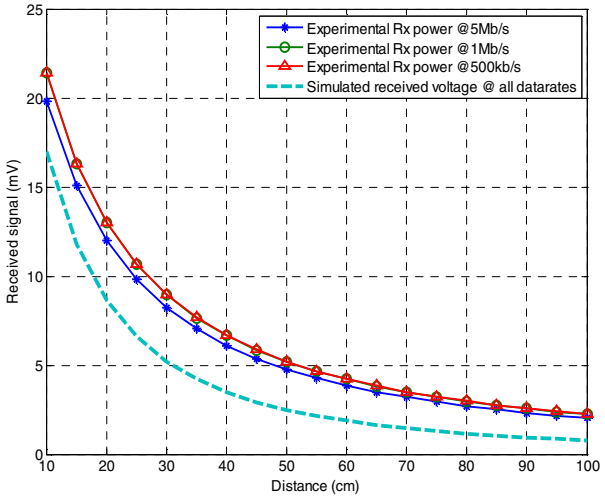

Figure 4. Experimental and. simulated received voltage along distance

As predicted, the voltage decreases as the distance increases. As discussed in the numerical analysis in Sec. II, the bandwidth has no effect on the received power, and thus the received voltage. For this reason, the simulation for all data rates is the same. For the same reason, the experimental received voltage values for the different data rates (500 kb/s,

1Mb/s and 5 Mb/s) are nearly following the same response with a deviation less than 1 mV. This deviation can be explained as a result of repeating the experiment for each data rate, which results in measurement errors but within the acceptable range. The deviation between simulation and experimental results is that the measurements taken are curve fitted to suit the Lambertian model. The curve fit does not represent the real measured values, instead it smoothens the response.

In order to study the system performance, the eye diagram is taken as a measure for BER. In Figs. 5(a-d), eye diagrams for a distance of 10 cm are drawn at 5 Mb/s and 1 Mb/s, before and after using a low pass filter. It is clear that the low pass filter has an important role in noise removal, and thereby increasing signal to noise ratio (SNR). Q-factor is taken as a measure of BER; whereas the Q-factor increases, BER decreases. For a reliable link with BER≤10^{-9}, the Q-factor nearly equals 6. At 1 Mb/s; before using the filter, Q=6.82 while after using it Q=18.337. For the 5 Mb/s, Q=5.8896 before the filter, and Q=15.65 after the filter. This gives a good performance measure for a 10 cm link for data rates up to 5 Mb/s. The link exhibits nearly error free transmission with and without filter.

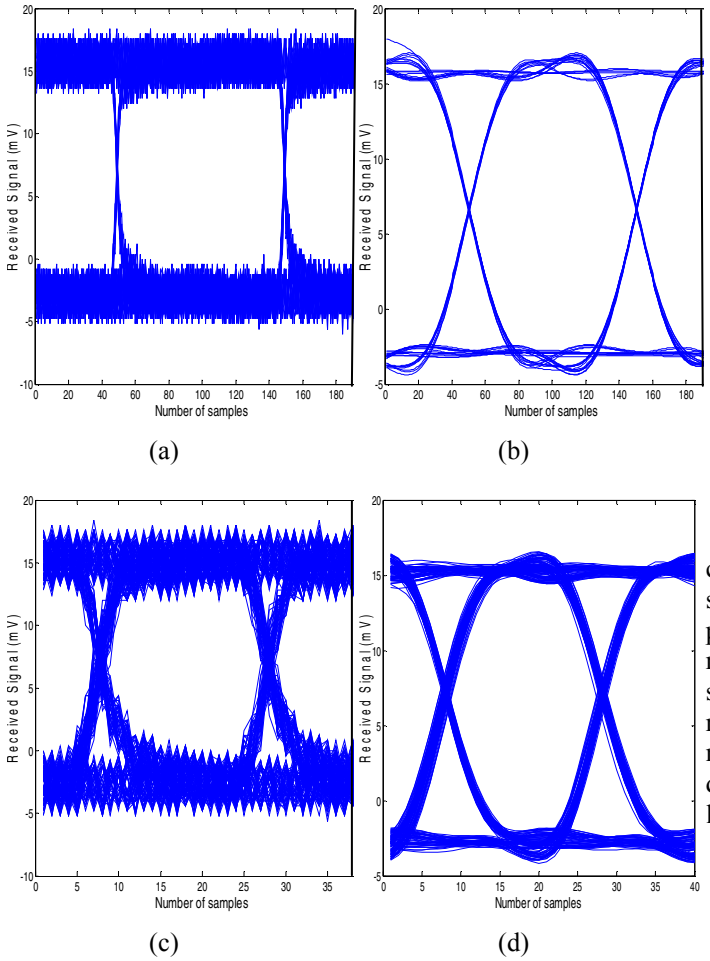

Figure 5. Eye patterns at a distance 10 cm for 1 Mb/s (a) without filter (b) with filter and 5Mb/s (c) without filter (d) with filter

When the distance increases to 100 cm, the results change dramatically, which are presented in Figs. 6(a-d). For 1 Mb/s, not using a filter results in a high BER, with Q=1.74. On the other hand, using a filter results in Q=11.29 with BER above the required limit. When the data rate increases to 5 Mb/s, Q=1.62 without filter and Q=8.33 after filter.

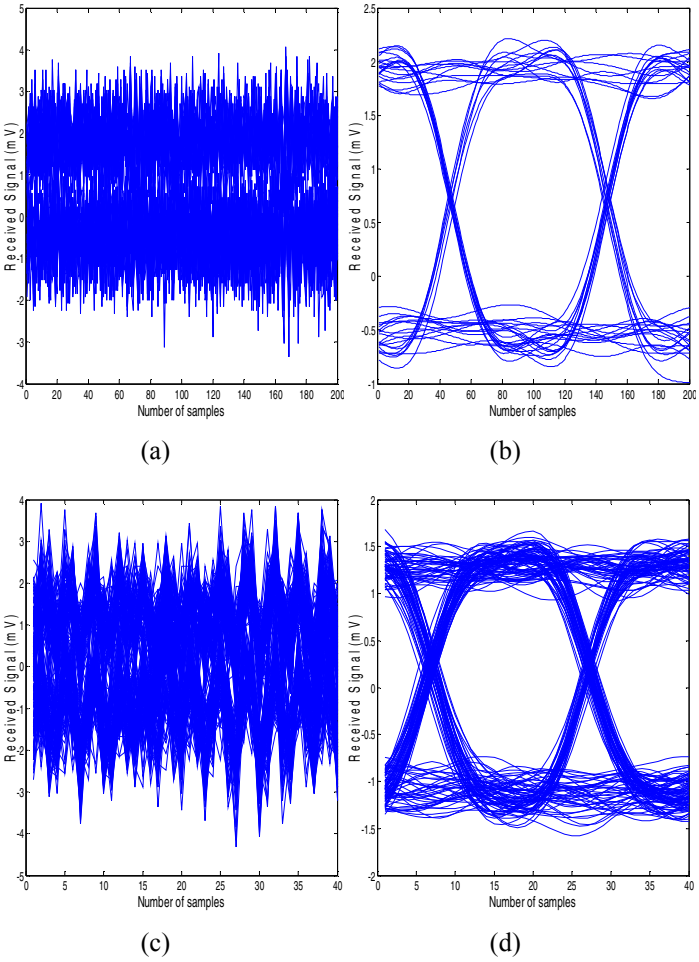

Figure 6. Eye patterns at a distance 100 cm for 1 Mb/s (a) without filter (b) with filter and 5Mb/s (c) without filter (d) with filter

In Fig. 7, the different noise sources discussed in Sec. II are considered in simulating the received power. The power sensitivity limits for each data rate at BER threshold of 10^{-9} is plotted. The sensitivity threshold indicates the minimum received power to achieve a reliable BER. In this case the sensitivity lies between -37 dBm and -43 dBm. As shown, the received power is far above the boundary limits. The minimum received power level at the 100 cm distance is -25 dBm, and thus indicating much lower BER than the threshold limit.

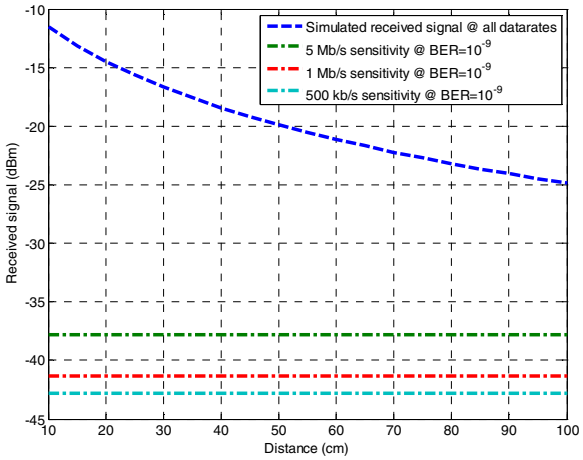

Figure 7. Simulated received signal (dBm) along distance compared with optical sensitivity

V. CONCLUSIONS

In this paper an experimental investigation is implemented for a short (1 m) FSO link for three different data rates up to 5 Mb/s. A transmitter and a receiver are designed and implemented then the experiment is modelled using a ray trace model. The system performance is studied for theoretical BER calculated from received signal frames and compared with the power sensitivity threshold to achieve BER of 10^{-9}.

Results have shown a high performance with Q-factor above 8 for the worst case after using a low pass filter. This Q-factor value indicates BER $\leq 10^{-9}$. Simulation results validate the experimental results after modelling different noise parameters. The minimum received power is -25 dBm and the power sensitivity range lies between -37 and -43 dBm.

REFERENCES

[1] W. O. Popoola, "Subcarrier intensity modulated free-space optical communication systems," Phd dissertation, University of Northumbria, Newcastle, England, Sep. 2009.

[2] David A. Johnson, *Handbook of optical through the air communications* [online]. Available: http://www.imagineeringezine.com/air-bk2.html [Access: 1 Nov. 2015].

[3] Z. Ghassemlooy, W. Popoola, and S. Rajbhandari, "Channel modelling," Optical wireless communications: system and channel modelling with Matlab, Boca Raton, FL: CRC Press, 2012, Ch. 3, Sec. 3.1, pp. 77-84.

[4] *Photodiode Characteristics and Applications,* Osioptoelectronics [online]. Available: *http*://www.osioptoelectronics.com/application-notes/AN-Photodiode-Parameters-Characteristics.pdf [Access: 29 Sep. 2015].

[5] Xavier Ramus, "Transimpedance considerations for high-speed amplifiers," Texas Instruments, 2009 [online]. Available: http://www.ti.com/lit/an/sboa122/sboa122.pdf [Access: 1 Nov. 2015].

[6] Govind P. Agrawal, "Optical receivers," Fiber-optic communication systems, Wiley-Interscience, 2002, Ch.4, pp. 164-167.

[7] Carl Brännlund, "High speed electronics for free space optical communication between spacecraft," M Sc. dissertation (Uppsala University, Sweden 2008) [online]. Available: http://www.researchgate.net/publication/242742423_High_Speed_Electronics_for_Free_Space_Optical_Communication_between_Spacecraft [Access: 1 Nov. 2015].

[8] *2N4401/ MMBT4401 NPN General-purpose amplifier,* Fairchild, 2014 [online]. Available: https://www.fairchildsemi.com/datasheets/2N/2N4401.pdf [Access: 3 Nov. 2015].

[9] *Ultralow distortion, high speed 0.95 nV/√Hz voltage noise op amp AD8099,* Analog, 2013 [online]. Available: http://www.analog.com/media/en/technical-documentation/data-sheets/AD8099.pdf [Access: 2 Nov. 2015].

[10] *High power infrared emitter (850 nm) SFH4350,* Osram, 2014 [online]. Available: http://www.osram-os.com/osram_os/en/products/product-catalog/infrared-emitters%2c-detectors-andsensors/infrared-emitters/power-emitter-gt40mw/emitter-with-850-nm/sfh-4350/index.jsp [Access: 4 Nov. 2015].

[11] *Silicon PIN photodiode with very short switching time SFH 203 PFA,* Osram, 2003 [online]. Available: http://www.osram-os.com/Graphics/XPic8/00029214_0.pdf/SFH%20203%20P,%20SFH%20203PFA.pdf [Access: 1 Nov. 2015].